

1 **Viability RT-PCR for SARS-CoV-2: a step forward to solve the infectivity quandary**

2  
3 Enric Cuevas-Ferrando, MSc<sup>1</sup>; Walter Randazzo, PhD<sup>1</sup>; Alba Pérez-Cataluña, PhD<sup>1</sup>; Irene  
4 Falcó, MSc<sup>1</sup>; David Navarro, PhD<sup>2,3</sup>; Sandra Martin-Latin, PhD<sup>4</sup>; Azahara Díaz-Reolid,  
5 MSc<sup>1</sup>; Inés Girón-Guzmán, BSc<sup>1</sup>; Ana Allende, PhD<sup>5</sup>; Gloria Sánchez, PhD<sup>1\*</sup>

6  
7 <sup>1</sup>Department of Preservation and Food Safety Technologies, Institute of Agrochemistry  
8 and Food Technology, IATA-CSIC, Av. Agustín Escardino 7, Paterna, 46980, Valencia,  
9 Spain

10 <sup>2</sup>Microbiology Service, Clinic University Hospital, INCLIVA Health Research Institute,  
11 Valencia, Spain

12 <sup>3</sup>Department of Microbiology, School of Medicine, University of Valencia, Valencia,  
13 Spain

14 <sup>4</sup>Université Paris-Est, ANSES Laboratory for Food Safety, Maisons-Alfort, F-94700, France

15 <sup>5</sup>Research Group on Quality and Safety of Fruits and Vegetables, Department of Food  
16 Science and Technology, CEBAS-CSIC, Campus Universitario de Espinardo, 25, 30100,  
17 Murcia, Spain

18  
19 \*Corresponding author

20 Correspondence to: [gloriasanchez@iata.csic.es](mailto:gloriasanchez@iata.csic.es)

21 **Summary**

22 **Background:** Isolation, contact tracing and restrictions on social movement are being globally  
23 implemented to prevent and control onward spread of SARS-CoV-2, even though the infection  
24 risk modelled on RNA detection by RT-qPCR remains biased as viral shedding and infectivity are  
25 not discerned. Thus, we aimed to develop a rapid viability RT-qPCR procedure to infer SARS-CoV-  
26 2 infectivity in clinical specimens and environmental samples. **Methods:** We screened  
27 monoazide dyes and platinum compounds as viability molecular markers on five SARS-CoV-2  
28 RNA targets. A platinum chloride-based viability RT-qPCR was then optimized using genomic  
29 RNA, and inactivated SARS-CoV-2 particles inoculated in buffer, stool, and urine. Our results  
30 were finally validated in nasopharyngeal swabs from persons who tested positive for COVID-19  
31 and in wastewater samples positive for SARS-CoV-2 RNA. **Findings:** We established a rapid  
32 viability RT-qPCR that selectively detects potentially infectious SARS-CoV-2 particles in complex  
33 matrices. In particular, the confirmed positivity of nasopharyngeal swabs following the viability  
34 procedure suggests their potential infectivity, while the complete prevention of amplification in  
35 wastewater indicated either non-infectious particles or free RNA. **Interpretation:** The viability  
36 RT-qPCR approach provides a more accurate ascertainment of the infectious viruses detection  
37 and it may complement analyses to foster risk-based investigations for the prevention and  
38 control of new or re-occurring outbreaks with a broad application spectrum. **Fundings:** This work  
39 was supported by Spanish Scientific Research Council (CSIC), Generalitat Valenciana, and  
40 MICINN co-founded by AEI/FEDER, UE.

## 41 Introduction

42 The rapid spread of severe acute respiratory syndrome coronavirus 2 (SARS-CoV-2) has led to  
43 an unprecedented global health and economic crisis. SARS-CoV-2 belongs to the *Coronaviridae*  
44 family, which includes enveloped RNA viruses causing respiratory, enteric, and systemic  
45 infections in a wide range of hosts, including humans and animals. Human coronaviruses have  
46 been traditionally considered responsible for endemic infections causing common cold  
47 symptoms, as in the cases of HKU1, 229E, OC43, and NL63 viruses, while more recently Middle  
48 East respiratory syndrome coronavirus (MERS-CoV) and SARS-CoV produced more severe  
49 epidemics in the Arabian Peninsula and in Asia. COVID-19 symptoms range from mild to severe,  
50 in which severe pneumonia and respiratory distress syndrome can lead to death. However, a  
51 significant number of infected people are asymptomatic, making the epidemiological control  
52 even more challenging.

53 SARS-CoV-2 is an airborne human pathogen primarily transmitted through droplets and  
54 aerosols, even though its detection in urine and faecal specimens raised the hypothesis of the  
55 possible fecal-oral transmission further sustained by the successful viral replication in cell  
56 culture.<sup>(1,2)</sup> To control SARS-CoV-2 spread, extreme containment measures have been enforced  
57 worldwide along with several epidemiological surveillance strategies, which include tracing  
58 confirmed and suspected cases by clinical testing (e.g., SARS-CoV-2 nucleic acid or antigen tests  
59 on nasal or oral swabs or saliva samples), and monitoring community transmission by  
60 wastewater analysis (known as Wastewater Based Epidemiology, WBE).<sup>(3)</sup>

61 In this context, several molecular assays based on real-time reverse transcriptase polymerase  
62 chain reaction (RT-qPCR) have been developed to detect and quantify SARS-CoV-2 RNA in clinical  
63 and environmental samples. For instance, a test-based strategy (at least two consecutive  
64 negative RT-qPCR tests) has been widely adopted as a general public health guidance for release  
65 from (self-) isolation, reincorporation into the workplace, and patient transferral. However,  
66 COVID-19 patients can continue to shed viral RNA well beyond clinical recovery and persistent  
67 positive RT-qPCR does not necessarily indicate infectiousness.<sup>(4)</sup> Besides being a rapid, easy-to-  
68 use, and cost-effective technique, RT-qPCR informs on the presence of viral RNA that does not  
69 correlate with infectivity, yet such testing is still being used as a surrogate marker of infectivity.<sup>(5-  
70 8)</sup> On the contrary, viral replication in permissive cell line(s) represents the conclusive evidence  
71 to assess viral infectivity, and it has been readily available for SARS-CoV-2. Conversely, the facility  
72 requirements needed to handle SARS-CoV-2 infectious materials (biosafety level 3 laboratory,  
73 BSL-3), in addition to the low sensitivity and long turnaround time for results, typically from  
74 three to ten days, limited its extensive implementation for both clinical diagnosis and  
75 environmental risk assessment.<sup>(9)</sup>

76 Recently, novel molecular techniques, referred to as capsid integrity or viability qPCR assays  
77 incorporating viability markers such as monoazide dyes and metal compounds into qPCR-based  
78 methods, have been demonstrated to selectively remove false-positive qPCR signals deriving  
79 from free nucleic acids and virions with damaged capsids, finally allowing an estimation on viral  
80 infectivity.<sup>(10)</sup> However, the application of such techniques for enveloped viruses has not fully  
81 elucidated as it has failed for avian influenza virus (IAV) and infectious laryngotracheitis virus  
82 (ILTIV) while it has recently been optimized for porcine epidemic diarrhea coronavirus.<sup>(11-13)</sup>  
83 Nonetheless, the implementation of this technique has not been explored for SARS-CoV-2.

## 84 Methods

### 85 ***Viral materials, viability markers and optimization of viability treatment***

86 SARS-CoV-2 genomic RNA (VR-1986D™, ATCC, VA, US), gamma-irradiated ( $5 \times 10^6$  RADs)  
87 (NRC-52287, BEI Resources, VA, US) and heat inactivated (65°C for 30 min) (NR-52286, BEI  
88 Resources, VA, US) viral particles preparations all obtained from isolate USA-WA1/2020 were  
89 used for initial screening of viability markers. Specifically, monoazide photoactivatable dyes and  
90 platinum compounds were initially screened as viability marker candidates using SARS-CoV-2  
91 genomic RNA, gamma-inactivated, and heat inactivated SARS-CoV-2 suspensions. Viability  
92 marker stock solutions were prepared as follows and stored at -20 °C for later use: ethidium

93 monoazide (EMA<sup>™</sup>, Geniul, Spain) was diluted in dimethylsulfoxide (DMSO) to 2.0 mM, PEMAX<sup>™</sup>  
94 (Geniul, Spain) and propidium monoazide (PMAxx<sup>™</sup>, Biotium, CA, US) were diluted in nuclease-  
95 free water to 4.0 mM, platinum (IV) chloride (PtCl<sub>4</sub>; Acros Organics, NJ, US) and cis-  
96 diamineplatinum (II) dichloride (CDDP; Sigma-Aldrich, MO, US) salts were dissolved in DMSO to  
97 1.0 M and further diluted in nuclease-free water to 50 mM. Viability assays were carried out by  
98 treating 300 µL of either genomic SARS-CoV-2 RNA (approx. 10<sup>3</sup> gc/mL), gamma-inactivated  
99 (approx. 10<sup>5</sup> gc/mL), and heat inactivated SARS-CoV-2 (approx. 10<sup>5</sup> gc/mL) suspensions with final  
100 concentrations of 50-100 µM photoactivatable dyes (PMAxx<sup>™</sup>, PEMAX<sup>™</sup>, or EMA<sup>™</sup>) or 0.1-2.0  
101 mM platinum compounds (CDDP or PtCl<sub>4</sub>) in DNA LoBind tubes (Eppendorf, Germany).  
102 Photoactivation of monoazide dyes was achieved by 10 min of dark-incubation in an orbital  
103 shaker (150 rpm) at room temperature (RT) followed by 15 min blue LED light exposure in a  
104 photo-activation system (Led-Active Blue, GenIUL). Alternatively, 30 min incubation at RT in an  
105 orbital shaker (150 rpm) were used for viability treatments with platinum compounds. A control  
106 consisting of genomic RNA or virus suspension without viability marker was included in each  
107 assay. Following the viability treatment, the viral RNA was immediately purified as described  
108 hereafter.

#### 109 ***Assessment of PtCl<sub>4</sub> viability RT-qPCR in artificially inoculated and validation in naturally*** 110 ***contaminated samples***

111 Platinum (IV) chloride was selected as the most reliable viability marker and tested at final  
112 concentrations of 0.5 to 5.0 mM for viability RT-qPCR optimization in stool, urine,  
113 nasopharyngeal swabs and wastewater samples.

114 For the initial optimization, stool and urine specimens that had tested negative for SARS-CoV-2  
115 were retrieved from IATA biobank. Faecal material was resuspended 1% w/v in phosphate-  
116 buffered saline (PBS), and supernatant recovered by centrifugation at 2000 × g for 5 min. Direct  
117 and ten-fold diluted urine, and ten-fold diluted faecal suspension (final 1% w/v faecal dilution)  
118 were spiked with either gamma- and/or heat inactivated SARS-CoV-2 to approximately 10<sup>5</sup> gc/L  
119 final concentration.

120 Then, nasopharyngeal swabs from positive COVID-19 patients and naturally contaminated  
121 wastewater samples were used to validate the viability PtCl<sub>4</sub> RT-qPCR. Nasopharyngeal swabs  
122 (n=9) from COVID-19 positive patients were originally collected at Hospital Clínico Universitario  
123 de Valencia (Valencia, Spain) and included in this study once de-identified. To test whether the  
124 detection of viral RNA was exclusive for infectious particles, nasopharyngeal swab subsamples  
125 were inactivated at 95 °C for 10 min, included in the experiments along with naïve specimen and  
126 both assayed by RT-qPCR and viability PtCl<sub>4</sub> RT-qPCR.

127 SARS-CoV-2 positive wastewater grabbed samples (n=6) were collected in June-October, 2020  
128 from different wastewater treatments plants involved in a WBE monitoring programme. The  
129 samples were originally concentrated by an aluminium precipitation procedure and tested  
130 positive for at least two RT-qPCR targets (N1, IP4 or E gene).<sup>(14)</sup> To exclude additional viral  
131 inactivation due to the concentration procedure, wastewater were freshly concentrated by  
132 Centricon-Plus 70 centrifugal ultrafilters units with a cut-off of 100 kDa (Merk-Millipore, MA,  
133 US).<sup>(15)</sup> Samples were all diluted in PBS as specified. Viability treatment, RNA extraction and  
134 SARS-CoV-2 detection were carried out as hereafter detailed.

#### 135 ***Viral RNA purification and SARS-CoV-2 detection***

136 Viral RNA was extracted using Maxwell<sup>®</sup> RSC 16 instrument and Maxwell RSC Pure Food GMO  
137 and authentication kit (Promega, Spain) and detected by RT-qPCR targeting N1, N2, E gene, IP2  
138 and IP4 regions.<sup>(16)</sup> Viral RNA from nasopharyngeal samples was extracted using a KingFisher<sup>™</sup>  
139 Flex (Thermo Fisher Scientific) instead. Given the superior sensitivity of N1 RT-qPCR resulting  
140 from the initial screening, this target was used for subsequent determinations. Each RT-qPCR  
141 assay was performed in duplicate and included nuclease-free water as negative control, and  
142 SARS-CoV-2 complete genomic RNA (VR-1986D<sup>™</sup>, ATCC, VA, US), E gene plasmid (10006896,  
143 2019-nCoV\_E Positive Control from Charité/Berlin, IDT, Belgium) or N1/N2 plasmid (10006625,  
144 2019-nCoV\_N\_Positive Control from CDC, IDT, Belgium) as positive controls. Ten-fold RNA

145 dilutions were consistently tested to check RT-qPCR inhibition due to viability marker residues  
146 or inhibitory substances in the sample.

#### 147 **Statistical analysis**

148 All data were compiled from three independent experiments with at least two technical  
149 replicates for each variable. Data are presented as median  $\pm$  SD. Significant differences in median  
150 cycle threshold (Ct) were determined by using either one- or two way(s) ANOVA followed by  
151 Dunnett's multiple comparisons test on GraphPad Prism version 8.02 (GraphPad Software, US).  
152 Differences in means were considered significant when the p was  $<0.05$ .

### 153 **Results**

#### 154 **Initial assessment of viability markers and RT-qPCR assays**

155 With regard to the viability markers tested, platinum compounds were better at preventing PCR  
156 amplification of SARS-CoV-2 genomic RNA suspension than monoazide dyes, regardless of the  
157 RT-qPCR target (Figure 1). Compared to untreated RNA, significant differences were detected  
158 for PtCl<sub>4</sub> and CDDP treated samples in all the five RT-qPCR targets tested. While PtCl<sub>4</sub> completely  
159 prevented the RNA amplification for all replicates, it occurred in 5 out of 20 CDDP treated  
160 replicates targeting N1, N2 and IP4. Among photoactivatable dyes, 50  $\mu$ M PMAxx offered the  
161 best performance as it removed the signal in 8 replicates showing statistically significant  
162 differences for E gene, IP2 and IP4. An additional assay tested 100  $\mu$ M PMAxx on SARS-CoV-2  
163 genomic RNA without any improvement of the results with respect to 50  $\mu$ M PMAxx  
164 concentration (data not shown). EMA and PEMAx completely removed RT-qPCR signals in 2 out  
165 of 20 replicates. Given these preliminary results, we further assessed PMAxx and PtCl<sub>4</sub> effect on  
166 SARS-CoV-2 gamma- (ca.  $8.50 \times 10^5$  gc/mL corresponding to 140 TCID<sub>50</sub>/mL) and heat inactivated  
167 (ca.  $1.88 \times 10^5$  gc/mL corresponding to 80 TCID<sub>50</sub>/mL) viral particles by using N1 as the most  
168 sensitive RT-qPCR assay among all the compared targets. PMAxx at 50  $\mu$ M minimally reduced  
169 the PCR signals by 2.82 and 3.17 Cts with respect to the gamma- and heat inactivated controls,  
170 while the superior ability of PtCl<sub>4</sub> was confirmed for both gamma- and heat inactivated SARS-  
171 CoV-2 viral particles (Figure 2). A final concentration of 1.0 mM PtCl<sub>4</sub> was needed to consistently  
172 prevent the amplification of inactivated viruses by viability RT-qPCR. Thus, we further applied  
173 the PtCl<sub>4</sub> viability RT-qPCR to high concentrated gamma-inactivated viral suspensions (ca.  $8.50 \times$   
174  $10^6$  gc/mL). Results showed that 0.5 and 1.0 mM PtCl<sub>4</sub> reduced by 3.4 and 6.8 Cts compared to  
175 the control. Although significant statistical differences were detected for all treatments  
176 regardless of the concentration of the metal compound, only 2.0 mM PtCl<sub>4</sub> showed to  
177 consistently prevent signal amplification (only one positive out of 8 replicates, Ct=39.11).

#### 178 **Effect of sample complexity on viability RT-qPCR**

179 To determine the effect of sample matrix on viability RT-qPCR, we spiked 10-fold diluted stool  
180 suspensions (1% w/v final dilution) and urine specimen (10% v/v final dilution) with  
181 approximately  $10^5$  gc/mL gamma-inactivated SARS-CoV-2, and applied up to 5.0 mM PtCl<sub>4</sub> as  
182 viability marker. Compared to the untreated control, significant differences were observed for  
183 1.0 mM PtCl<sub>4</sub> in urine samples or 1.25 mM PtCl<sub>4</sub> in stool suspensions (Figure 3). However, a  
184 concentration of 5.0 mM was needed to completely remove the PCR signals in urine, while 2.5  
185 mM PtCl<sub>4</sub> prevented the amplification of 1 out of 8 replicates in stool. Although the complete  
186 inhibition of amplification signals was achieved to a limited extent, a sharp difference above one  
187 logarithm of genomic copies ( $\Delta$ Cts $\approx$ 3.3) was observed in stool and urine samples processed with  
188 1.25 and 3.75 mM PtCl<sub>4</sub>, respectively.

#### 189 **Viability RT-qPCR validation on positive clinical samples and naturally contaminated 190 wastewater**

191 Additional experiments were set up to validate viability PtCl<sub>4</sub> RT-qPCR on nasopharyngeal swabs  
192 from COVID-19 positive patients and on naturally contaminated wastewater samples. Initial  
193 experiments using undiluted samples achieved unsuccessful results (data not showed), thus  
194 both clinical and wastewater samples were ten-fold diluted in PBS buffer. Nine 10-fold diluted  
195 nasopharyngeal swabs and the corresponding heat-inactivated (95 °C for 10 min) subsamples  
196 were processed by RT-qPCR alone and viability RT-qPCR with either 1.0 or 2.5 mM PtCl<sub>4</sub> (Figure

197 4). Applying 1.0 mM PtCl<sub>4</sub> viability RT-qPCR, consistent amplification signals were observed in  
198 both naïve and heat-treated samples with minimal Ct differences compared to RT-qPCR alone.  
199 Increased concentration to 2.5 mM led to a sharper discrimination of PCR signals ( $\Delta C_t = 9.24 \pm$   
200  $3.59$ ). Similarly, the complete prevention of RT-qPCR signals occurred in one out of four samples  
201 at 1.0 mM PtCl<sub>4</sub>, and in three out of five samples at 2.5 mM (Figure 4). Regardless of the viability  
202 marker concentration applied, the complete prevention of amplification was observed in  
203 samples with initial low viral titer (Ct values  $\geq 30$ ). Moreover, the 2.5 mM PtCl<sub>4</sub> viability RT-qPCR  
204 was further validated on six wastewater samples naturally contaminated with SARS-CoV-2. The  
205 results showed that 2.5 mM PtCl<sub>4</sub> completely prevented the amplification in all samples (Figure  
206 5).

## 207 Discussion

208 Currently, research projects aiming to assess the risk of transmission and exposure to infectious  
209 virus either in clinical and environmental settings have been limited by the biosafety level-3 (BSL-  
210 3) conditions needed to handle infectious SARS-CoV-2. The research effort of this investigation  
211 intended to provide a rapid and sensitive analytical method that selectively detects potentially  
212 infectious SARS-CoV-2 in a significantly shorter time than the traditional cell-culture based  
213 method and that can be used in a wide range of applications, including clinical and  
214 environmental COVID-19 monitoring programs as epidemiological response to the pandemic  
215 that is causing such a public health emergency.

216 This study evaluated photoactivatable monoazide dyes and metal compounds as viability  
217 markers applied prior to nucleic acid extraction to prevent amplification of RNA from non-viable  
218 viral particles, thus enabling amplification only of viable/infectious viruses in downstream RT-  
219 qPCR assay. Selecting platinum chloride as the best performing viability marker, we  
220 demonstrated that viability RT-qPCR efficiently discriminated free RNAs and inactivated SARS-  
221 CoV-2 inoculated in buffer, stool and urine suspensions. Then, we further proved that the  
222 method inferred SARS-CoV-2 infectivity better than RT-qPCR alone in both nasopharyngeal  
223 swabs from positive COVID-19 patients and in naturally contaminated wastewater samples. In  
224 the case of complex matrices, increased PtCl<sub>4</sub> concentration of 2.5 mM and ten-fold sample  
225 dilution are recommended because of the presence of suspended solids and inhibitors that  
226 hinder the efficacy of the viability treatment.

227 Our investigation initially included five well-established molecular assays since the length of the  
228 amplicon and/or the richness of secondary structures of targeted RNA may affect the efficiency  
229 of viability treatments.<sup>(17,18)</sup> We show that metal compounds performed better than monoazide  
230 dyes, irrespective of RT-qPCR assays. However, RT-qPCR targeting N1 region is recommended  
231 because of its superior sensitiveness. This aspect is of importance because complex matrices  
232 needed to be diluted to achieve a more efficient inference of viral infectivity, as demonstrated  
233 in spiked stool and urine, in positive swabs and in contaminated wastewater. Similarly, sample  
234 dilution was needed to implement a viability RT-qPCR targeting norovirus in sewage.<sup>(19)</sup>  
235 Moreover, N1 assay better fits the testing on samples with expected low viral concentrations  
236 (e.g., environmental samples) and/or PCR inhibitors (e.g., concentrated wastewater, stool). As  
237 N1 assay has been validated in many laboratories worldwide, this viability method could also be  
238 easily and widely implemented.

239 To the best of our knowledge, this is the first report on a rapid molecular assay independent  
240 from viral replication in cell culture developed to test SARS-CoV-2 infectivity. A recent  
241 investigation by our group demonstrated the suitability of viability RT-qPCRs to infer the  
242 infectivity of porcine epidemic diarrhea coronavirus, member of the genus *Alphacoronavirus*  
243 within *Coronaviridae* family.<sup>(13)</sup> Interestingly, we were able to demonstrate that PMAxx viability  
244 RT-qPCR matched the thermal inactivation pattern obtained by cell culture better than other  
245 viability markers, including PtCl<sub>4</sub>, and RT-qPCR alone.

246 Alternative rapid methods to assess the viability of enveloped viruses have been explored with  
247 unsuccessful results. These included propidium monoazide and immunomagnetic separation  
248 tested on laryngotracheitis virus and ethidium monoazide on avian influenza virus.<sup>(11,12)</sup> It is

249 worth to report that we also tested on inactivated SARS-CoV-2 suspensions a porcine gastric  
250 mucine *in situ* capture RT-qPCR, a method that was originally implemented in our laboratory for  
251 human enteric viruses.<sup>(20)</sup> Although proper SARS-CoV-2 infectious controls could not be included,  
252 those experiments resulted in inconclusive outcomes (data not shown).

253 Our viability RT-qPCR results of nasopharyngeal swabs from positive COVID-19 patients indicate  
254 the potential infectivity of the samples, while naturally contaminated wastewater are unlikely  
255 to contain infectious viral particles. These later findings reflect the viral replication in cell culture  
256 from RNA positive stool and respiratory samples as well as the unsuccessful attempts to isolate  
257 and cultivate SARS-CoV-2 from wastewater samples.<sup>(21-23)</sup>

258 Our findings are clinically relevant as RT-qPCR has become the primary method to diagnose  
259 COVID-19. However, as it detects RNA, its ability to determine the infectivity of patients is  
260 limited.<sup>(5-8)</sup> In addition, the immune system can neutralise SARS-CoV-2 preventing subsequent  
261 infection but not eliminating nucleic acid, which degrades slowly over time. This has been  
262 confirmed in cohort studies that concluded that seroconversion does not necessarily lead to the  
263 elimination of viral RNA, with cases being RT-PCR positive up to > 63 days after symptom onset  
264 despite having neutralizing antibodies.<sup>(24-26)</sup> Furthermore, some reports correlated the  
265 infectiousness of upper respiratory tract samples with RT-qPCR Ct values in COVID-19 cases.  
266 Analysing a large dataset (n=324), Singanayagam and colleagues demonstrated that the  
267 probability of viral recovery from samples with  $27.5 < Ct < 30$  was  $\approx 66\%$ , decreasing to  $\approx 28\%$  for  
268  $30 < Ct < 35$ , and to  $8-3\%$  for  $Ct > 35$ .<sup>(23)</sup> Similarly, Bullard observed SARS-CoV-2 cell infectivity  
269 only for respiratory specimens sampled < 8 days symptom onset with  $Ct < 24$ .<sup>(27)</sup> However, viral  
270 replication was also obtained from samples with elevated Ct values of 36-39.<sup>(7,28)</sup>

271 Notwithstanding, the correlation between RNA and virus isolation remains unclear.  
272 Unfortunately, we had no access to clinical samples with higher Ct values which are likely to  
273 contain non-infectious particles to contrast such hypothesis by the proposed viability RT-qPCR.  
274 In addition, the ratio between viral shedding and infectivity has been reported to vary along the  
275 course of the infection.<sup>(4,6,22)</sup> This information regarding epidemiological characteristics,  
276 symptom history and relevant sampling details included in medical records could have explained  
277 at least in part the different performances of viability RT-qPCR among clinical samples, however  
278 it could not be retrieved as de-identified specimens were analysed in this study.

279 Despite the viability treatment, we detected residual signals in heat inactivated nasopharyngeal  
280 swabs. This could be attributed to the viral envelop and nucleoproteins that limit the access  
281 and/or the binding of viability markers to SARS-CoV-2 RNA, as hypothesised for avian influenza  
282 virus and bacteriophage T4.<sup>(12,29)</sup> The enveloped structure of coronaviruses may also explain the  
283 increased concentration of viability markers needed for SARS-CoV-2 and PEDV compared to  
284 human enteric viruses.<sup>(13,19,30)</sup> This cumbersome finding obtained by the proposed viability  
285 procedure suggests that the overestimation of the infectivity of a given sample may occur which,  
286 although warranting a careful interpretation, represents a conservative prediction. With regards  
287 to wastewater samples that tested positive for SARS-CoV-2 RNA, they most probably contained  
288 detergents and chemicals that are detrimental to viral infectivity further supporting the efficacy  
289 of the viability RT-qPCR in discriminating potentially infectious and inactivated viral particles.<sup>(31)</sup>

290 The ultimate confirmation on the infectivity of the samples by cell culture, although  
291 recommendable, could not be provided. Detection of SARS-CoV-2 by either culture and viability  
292 RT-qPCR is valuable as a proxy for infectiousness; however, as the human infectious dose  
293 remains unknown, the significance of low titres of infectious virus for human-to-human  
294 transmission remains uncertain. Above all, as some individuals reportedly remain PCR positive  
295 weeks after SARS-CoV-2 infection recovery, knowing whether viral RNA in these persistent  
296 carriers is contagious provides key insights for quarantine policy, to safely discontinue self-  
297 isolation and contact tracing as essential public health measures to definitively prevent  
298 transmission.<sup>(6,26,32)</sup> Besides some limitations, the proposed viability RT-qPCR effectively reduced  
299 the amplification signals of non-infectious and free RNA of SARS-CoV-2 in complex matrices  
300 finally providing a better estimation of the infectiousness of samples. Thus, mathematical

301 models derived from laboratory scale experiments comparing viability RT-qPCR and viral  
302 replication could correlate viral load and infectivity, finally providing relevant tools of interest  
303 based on rapid molecular assay for prevention strategies and risk assessment.

#### 304 **Conclusions**

305 In conclusion, the use of pre-treatments to prevent RT-qPCR amplification of RNA from non-  
306 infectious SARS-CoV-2 using platinum chloride as a viability marker of infectivity was  
307 implemented in stool and urine samples and successfully validated in naturally contaminated  
308 wastewater samples, supporting the idea that SARS-CoV-2 present in sewage is not infectious.  
309 Residual amplification signals in nasopharyngeal swabs exposed to heat-inactivation  
310 overestimated the amount of viable virus, still providing a conservative interpretation of the  
311 infectiousness of the sample. Our study proposes a rapid analytical tool based on viability RT-  
312 qPCR to infer SARS-CoV-2 infectivity with potential application in risk assessment, and  
313 prevention and control in public health programmes.

#### 314 **Contributors**

315 GS, AA and WR conceived the study with input from AP-C, IF, SML and EC-F. EC-F, IF, AD-R, and  
316 IG-G led data acquisition. DN provided the nasopharyngeal swabs from COVID-19 positive  
317 patients. GS, EC-F, and WR led data analysis, interpretation, and visualisation. EC-F and WR  
318 wrote the draft report, and all other authors revised the report critically for important  
319 intellectual content. All authors critically reviewed and approved the final version of the  
320 manuscript.

#### 321 **Declaration of interests**

322 All authors declare no competing interests.

#### 323 **Acknowledgements**

324 The study was supported by CSIC (202070E101), Generalitat Valenciana (Covid\_19-SCI), MICINN  
325 co-founded by AEI/FEDER, UE (AGL2017-82909), and MICINN/AEI (PID2019-105509RJ-I00). EC-F  
326 is recipient of a predoctoral contract from the MICINN, Call 2018.

327 We thank Agustin Garrido Fernández and Andrea Lopez de Mota at IATA-CSIC for providing  
328 support in sample processing. We acknowledge Global Omnium S.L., NILSA, Aguas de Malaga,  
329 ESAMUR and FACSA for coordinating and managing wastewater sampling.

330



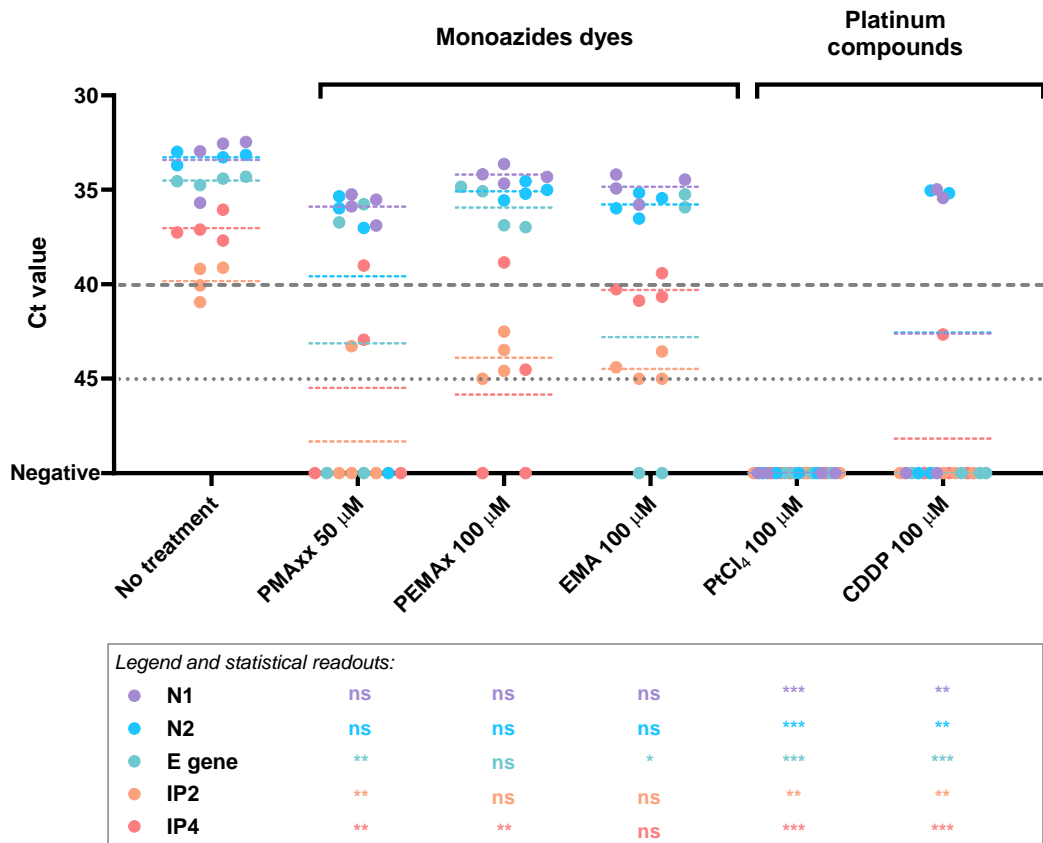
331  
332  
333  
334  
335  
336  
337  
338  
339  
340  
341  
342  
343  
344  
345  
346  
347  
348  
349  
350  
351  
352  
353  
354  
355  
356  
357  
358  
359  
360  
361  
362  
363  
364  
365  
366  
367  
368  
369  
370  
371  
372  
373  
374  
375  
376  
377  
378  
379  
380  
381  
382

## References

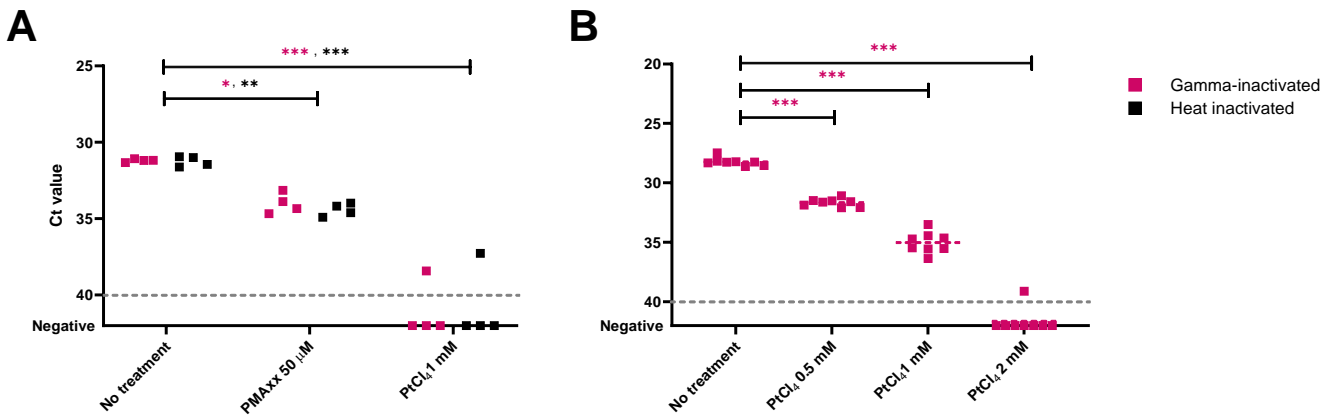
1. Meselson M. Droplets and aerosols in the transmission of SARS-CoV-2. *N Engl J Med* 2020; **382**:2063.
2. Guo M, Tao W, Flavell RA, Zhu S. Potential intestinal infection and faecal–oral transmission of SARS-CoV-2. *Nat Rev Gastroenterol Hepatol* 2021.
3. Bivins A, North D, Ahmad A, Ahmed W, Alm E, Been F, et al. Wastewater-Based Epidemiology: Global Collaborative to Maximize Contributions in the Fight against COVID-19. *Environ Sci Technol* 2020; **13**:7754–7.
4. Owusu D, Pomeroy MA, Lewis NM, Wadhwa A, Yousaf AR, Whitaker B, et al. Persistent SARS-CoV-2 RNA Shedding without Evidence of Infectiousness: A Cohort Study of Individuals with COVID-19. *J Infect Dis* 2021; jia107.
5. Atkinson B, Petersen E. SARS-CoV-2 shedding and infectivity. *Lancet* 2020; **395**:1339–40.
6. Widders A, Broom A, Broom J. SARS-CoV-2: The viral shedding vs infectivity dilemma. *Infect Dis Heal* 2020; **25**:210–5.
7. Romero-Gómez MP, Gómez-Sebastian S, Cendejas-Bueno E, Montero-Vega MD, Mingorance J, García-Rodríguez J. Ct value is not enough to discriminate patients harbouring infective virus. *J Infect* 2021; **20**:30720-9.
8. Krupp K, Madhivanan P, Perez-Velez CM. Should qualitative RT-PCR be used to determine release from isolation of COVID-19 patients? *J Infect* 2020; **3**:452–82.
9. Ogando NS, Dalebout TJ, Zevenhoven-Dobbe JC, Limpens RWAL, van der Meer Y, Caly L, et al. SARS-coronavirus-2 replication in Vero E6 cells: Replication kinetics, rapid adaptation and cytopathology. *J Gen Virol* 2020; **9**:925–940.
10. Leifels M, Dan C, Sozzi E, Shoultz DC, Wuertz S, Mongkolsuk S, et al. Capsid integrity quantitative PCR to determine virus infectivity in environmental and food applications – A systematic review. *Water Res X* 2020; **11**:100080.
11. Bindari YR, Walkden-Brown SW, Gerber PF. Methods to prevent PCR amplification of DNA from non-viable virus were not successful for infectious laryngotracheitis virus. *PLoS ONE* 2020; **5**:e0232571.
12. Graiver DA, Saunders SE, Topliff CL, Kelling CL, Bartelt-Hunt SL. Ethidium monoazide does not inhibit RT-PCR amplification of nonviable avian influenza RNA. *J Virol Methods* 2010; **164**:51-4.
13. Puente H, Randazzo W, Falcó I, Carvajal A, Sánchez G. Rapid Selective Detection of Potentially Infectious Porcine Epidemic Diarrhea Coronavirus Exposed to Heat Treatments Using Viability RT-qPCR. *Front Microbiol* 2020; **11**:1911.
14. Randazzo W, Truchado P, Cuevas-Ferrando E, Simón P, Allende A, Sánchez G. SARS-CoV-2 RNA in wastewater anticipated COVID-19 occurrence in a low prevalence area. *Water Res* 2020; **181**:115942.
15. Medema G, Heijnen L, Elsinga G, Italiaander R, Brouwer A. Presence of SARS-Coronavirus-2 RNA in Sewage and Correlation with Reported COVID-19 Prevalence in the Early Stage of the Epidemic in The Netherlands. *Environ Sci Technol Lett* 2020; acs.estlett.0c00357.
16. Pérez-Cataluña A, Cuevas-Ferrando E, Randazzo W, Falcó I, Allende A, Sánchez G. Comparing analytical methods to detect SARS-CoV-2 in wastewater. *Sci Total Environ* 2021; **758**:143870.
17. Contreras PJ, Urrutia H, Sossa K, Nocker A. Effect of PCR amplicon length on suppressing signals from membrane-compromised cells by propidium monoazide treatment. *J Microbiol Methods* 2011; **1**:89–95.
18. Soejima T, Schlitt-Dittrich F, Yoshida S-I. Polymerase chain reaction amplification length-dependent ethidium monoazide suppression power for heat-killed cells of Enterobacteriaceae. *Anal Biochem* 2011; **1**:37–43.
19. Randazzo W, López-Gálvez F, Allende A, Aznar R, Sánchez G. Evaluation of viability PCR performance for assessing norovirus infectivity in fresh-cut vegetables and irrigation water. *Int J Food Microbiol* 2016; **229**:1–6.

- 383 20. Falcó I, Randazzo W, Rodríguez-Díaz J, Gozalbo-Rovira R, Luque D, Aznar R, et al. Antiviral  
384 activity of aged green tea extract in model food systems and under gastric conditions. *Int J*  
385 *Food Microbiol* 2019; **292**:101–6.
- 386 21. Rimoldi SG, Stefani F, Gigantiello A, Polesello S, Comandatore F, Mileto D, et al. Presence  
387 and infectivity of SARS-CoV-2 virus in wastewaters and rivers. *Sci Total Environ* 2020;  
388 **744**:140911.
- 389 22. Wölfel R, Corman VM, Guggemos W, Seilmaier M, Zange S, Müller MA, et al. Virological  
390 assessment of hospitalized patients with COVID-2019. *Nature* 2020; **7809**:465–9.
- 391 23. Singanayagam A, Patel M, Charlett A, Lopez Bernal J, Saliba V, Ellis J, et al. Duration of  
392 infectiousness and correlation with RT-PCR cycle threshold values in cases of COVID-19,  
393 England, January to May 2020. *Euro Surveill* 2020; **32**:2001483.
- 394 24. Molina LP, Chow S-K, Nickel A, Love JE. Prolonged detection of Severe Acute Respiratory  
395 Syndrome Coronavirus 2 (SARS-CoV-2) RNA in an obstetric patient with antibody  
396 seroconversion. *Obstet Gynecol* 2020; **4**:838–41.
- 397 25. Liu W-D, Chang S-Y, Wang J-T, Tsai M-J, Hung C-C, Hsu C-L, et al. Prolonged virus shedding  
398 even after seroconversion in a patient with COVID-19. *J Infect* 2020; **2**:318–56.
- 399 26. Vibholm LK, Nielsen SSF, Pahus MH, Frattari GS, Olesen R, Andersen R, et al. SARS-CoV-2  
400 persistence is associated with antigen-specific CD8 T-cell responses. *EBioMedicine* 2021;  
401 **64**:103230.
- 402 27. Bullard J, Dust K, Funk D, Strong JE, Alexander D, Garnett L, et al. Predicting infectious  
403 SARS-CoV-2 from diagnostic samples. *Clin Infect Dis* 2020; ciaa638.
- 404 28. Clinical and virologic characteristics of the first 12 patients with coronavirus disease 2019  
405 (COVID-19) in the United States. *Nat Med* 2020; **6**:861–8.
- 406 29. Fittipaldi M, Rodriguez NJP, Codony F, Adrados B, Peñuela GA, Morató J. Discrimination of  
407 infectious bacteriophage T4 virus by propidium monoazide real-time PCR. *J Virol Methods*  
408 2010; **168**:228–32.
- 409 30. Randazzo W, Vasquez-García A, Aznar R, Sánchez G. Viability RT-qPCR to distinguish  
410 between HEV and HAV with intact and altered capsids. *Front Microbiol* 2018; **9**:1973.
- 411 31. Khokhar M, Roy D, Purohit P, Goyal M, Setia P. Viricidal treatments for prevention of  
412 coronavirus infection. *Pathog Glob Health* 2020; **7**:349–59.
- 413 32. Esteve C, Catherine FX, Chavanet P, Blot M, Piroth L. How should a positive PCR test result  
414 for COVID-19 in an asymptomatic individual be interpreted and managed? *Med Mal Infect*  
415 2020; **8**:633–638.

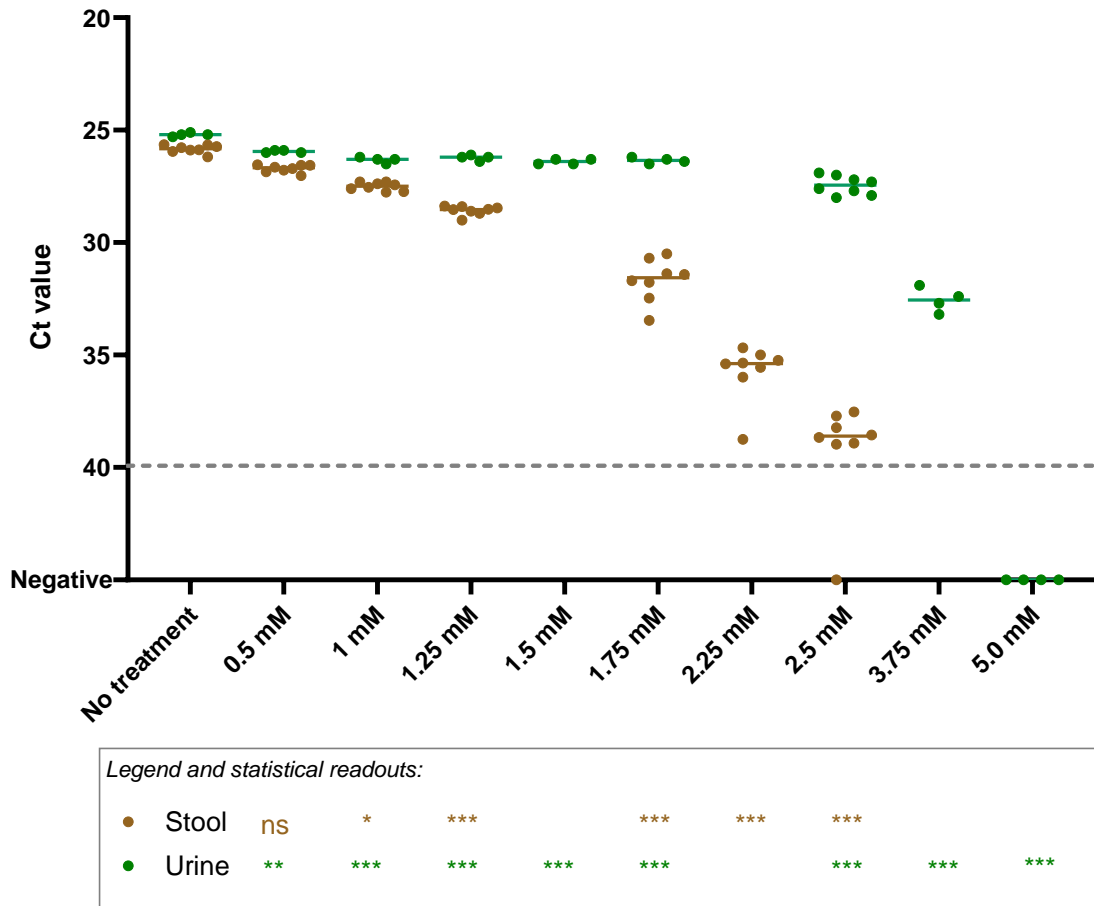
416 **Figure 1.** Performance of monoazide photoactivatable dyes and platinum compounds on SARS-  
 417 CoV-2 genomic RNA assessed by targeting five different RNA regions. Dashed grey line  
 418 represents RT-qPCR theoretical limit of detection for N1, N2 and gen E; dotted grey line  
 419 represents RT-qPCR theoretical limit of detection for IP2 and IP4. Asterisks indicate significant  
 420 difference from untreated control for each molecular target: ns, not significant; \*p<0.01;  
 421 \*\*p<0.001; \*\*\*p<0.0001; ns, not significant.



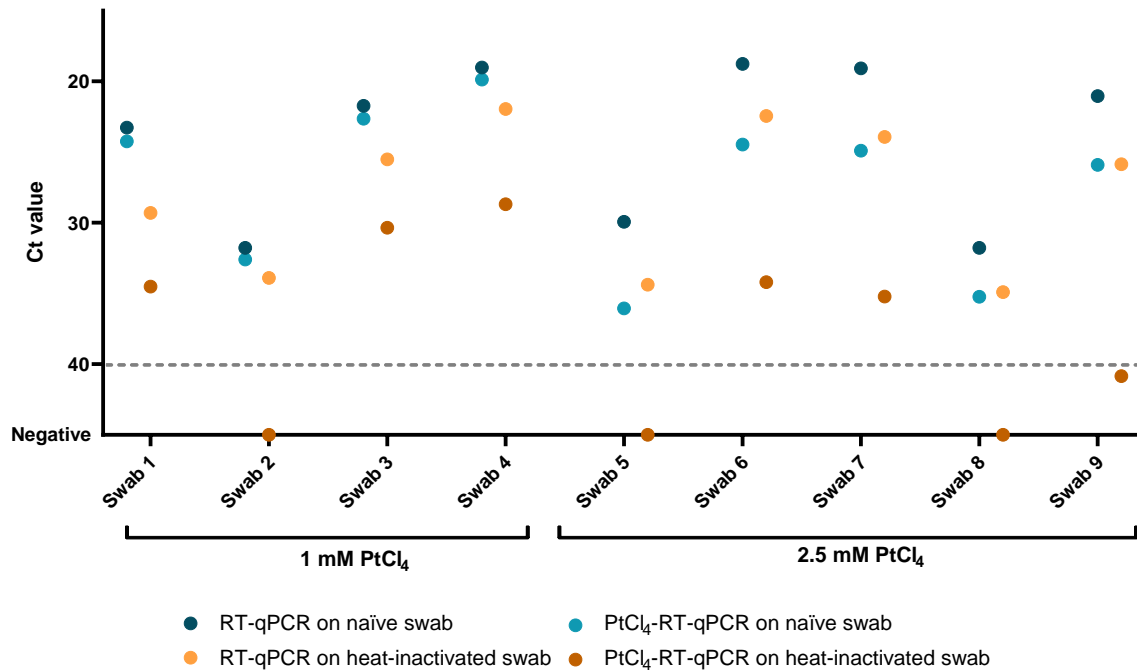
422 **Figure 2.** Assessment of viability markers on inactivated SARS-CoV-2 viral particles suspended in  
 423 PBS buffer at different concentrations. RT-qPCR assays targeted N1 region. A) Comparison of  
 424 PMAxx and platinum chloride (PtCl<sub>4</sub>) viability RT-qPCRs on low (ca. 10<sup>3</sup> gc/mL) gamma- and heat  
 425 inactivated SARS-CoV-2 viral particles. B) Viability RT-qPCR optimization using increasing  
 426 concentration of PtCl<sub>4</sub> on high concentrations of gamma-inactivated SARS-CoV-2 viral particles  
 427 (ca. 10<sup>5</sup> gc/mL). Dashed grey lines represent RT-qPCR theoretical limit of detection. Asterisks  
 428 indicate significant difference from untreated control: \*p<0.01; \*\*p<0.001; \*\*\*p<0.0001.



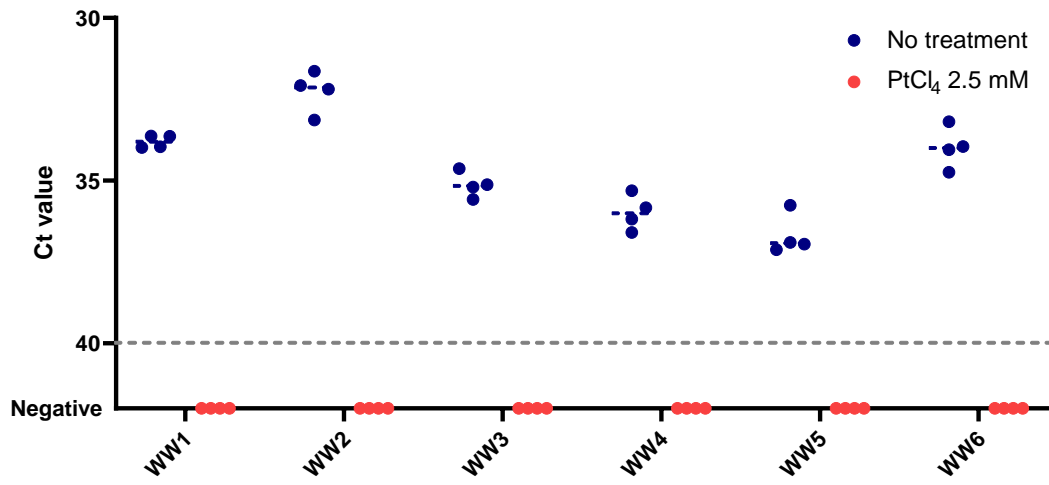
429 **Figure 3.** Platinum chloride (PtCl<sub>4</sub>) viability RT-qPCR on ten-fold diluted faecal suspensions (1%  
 430 w/v final dilution) (brown dots) and urine specimens (10% v/v final dilution) (green dots) spiked  
 431 with approximately 10<sup>5</sup> gc/mL gamma-inactivated SARS-CoV-2. Dashed grey line represents RT-  
 432 qPCR theoretical limit of detection. Asterisks indicate significant difference from untreated  
 433 control: \*p<0.01; \*\*p<0.001; \*\*\*p<0.0001; ns, not significant.



434 **Figure 4.** Validation of viability RT-qPCR with either 1mM or 2.5 mM PtCl<sub>4</sub> on ten-fold diluted  
 435 nasopharyngeal swabs from COVID-19 positive patients. Plotted dots represents the median  
 436 cycle threshold value (Ct) of naïve and heat-inactivated (95 °C for 10 min) subsamples assayed  
 437 by RT-qPCR alone and viability RT-qPCR both targeting N1. Dashed grey line represents RT-qPCR  
 438 theoretical limit of detection.



439 **Figure 5.** Validation of 2.5 mM PtCl<sub>4</sub> viability RT-qPCR on ten-fold diluted naturally contaminated  
440 wastewater samples. Dashed grey line represents RT-qPCR theoretical limit of detection.



441 **Research in context**

442 **Evidence before this study**

443 Previous works have established RT-qPCR methods for the efficient detection of severe acute  
444 respiratory syndrome coronavirus 2 in stool, urine and respiratory samples, with the latter being  
445 the most commonly used specimens in tracing COVID-19 cases. Similarly, wastewater-based  
446 epidemiology has been globally implemented to monitor the community spread of the virus.  
447 However, SARS-CoV-2 RNA load in clinical and environmental samples is not indicative of  
448 infectiousness. The distinction between viral shedding and infectivity is important for the  
449 development of prevention policy and quarantine guidelines as well as for the assessment of  
450 the risk of contamination in environmental settings. Some reports correlated RT-PCR Ct value  
451 and culture positivity and there is scientific evidence that persistent PCR positive individuals are  
452 not transmitting at the post-symptomatic stage of infection. However, testing viral replication is  
453 not feasible for large scale clinical screening or for environmental surveillance. In addition, the  
454 biosafety level 3 laboratory requirements needed to handle SARS-CoV-2 infectious materials and  
455 the turnaround time for culture results has also limited investigation on related topics. Previous  
456 works have established rapid viability assays based on RT-qPCR pre-treatments to infer the  
457 potential infectivity of enteric viruses, including norovirus, hepatitis A and E viruses in  
458 environmental and food samples. Unsuccessful attempts were reported for influenza virus and  
459 infectious laryngotracheitis virus, while a viability RT-qPCR for the selective detection of  
460 infectious and heat-inactivated porcine epidemic diarrhea coronavirus, as an enveloped viral  
461 model, was recently proposed. However, the sensitivity and reliability of this method remains  
462 to be shown for SARS-CoV-2.

463 **Added value of this study**

464 We show that SARS-CoV-2 RNA amplification of non-infectious samples can be reproducibly  
465 prevented by processing clinical and wastewater samples by a platinum chloride viability RT-  
466 qPCR technique. To the best of our knowledge this is the first report on this subject that also  
467 provides the following distinguishing features: (i) the procedure was optimized using standard  
468 materials which include SARS-CoV-2 genomic RNA, gamma- and heat inactivated viral particles;  
469 (ii) the preliminary findings were validated in nasopharyngeal swabs from COVID-19 positive  
470 patients and in wastewater samples naturally contaminated with SARS-CoV-2 RNA.

471 Overall, this study allows to selectively detect SARS-CoV-2 RNA belonging to potentially  
472 infectious viral particles in complex matrices of interest for epidemiological surveillance and  
473 pandemic control.

474 **Implications of all the available evidence**

475 Extensive lockdown measures are currently allowing to partially mitigate the spread of SARS-  
476 CoV-2. As such, it is of extreme importance to set up feasible and reliable epidemiological  
477 surveillance strategies that include clinical and environmental monitoring programs.  
478 Information on the infectivity of such samples is the keystone to better define the transmission  
479 route(s) and the risk of exposure. Further developments of predictive models based on such a  
480 viability approach may have a broad range of applications: including risk assessment, food safety  
481 and public health policy.